

# Two Paleoproterozoic Orogenies in the Evolution of the Tandilia Belt, Buenos Aires, as Evidenced by Zircon U-Pb SHRIMP Geochronology

LÉO AFRANEO HARTMANN,<sup>1</sup>

*Instituto de Geociências, Universidade Federal do Rio Grande do Sul, Avenida Bento Gonçalves, 9500; 91501-970 Porto Alegre, Rio Grande do Sul, Brazil*

JOÃO ORESTES S. SANTOS,

*Brazilian Geological Survey (CPRM), Rua Banco da Província, 105; 90840-030 Porto Alegre, Rio Grande do Sul, Brazil*

CARLOS A. CINGOLANI,

*Universidad Nacional de La Plata, calle 1 n. 644, 1900-La Plata, Argentina*

AND NEAL J. MCNAUGHTON

*Center for Global Metallogeny, The University of Western Australia, Perth 6907 WA, Australia*

## Abstract

The superposition of two orogenies during the evolution of the Paleoproterozoic Tandilia Belt, Argentina, produced complex geological structures in the granitic-gneissic-migmatitic Buenos Aires Complex. Ion microprobe (SHRIMP II) dating of 61 spots in 56 zircon crystals from 10 rock samples shows tectonic activity related to the accretionary Encantadas orogeny of 2.25–2.12 Ga, although a major overprint of the collisional Camboriú orogeny of 2.10–2.08 Ga is also recognized. Only one zircon age is Neoproterozoic. Two age peaks for the Tandilia Belt are ~2.16 Ga and ~2.08 Ga, which occur along most of the Brazilian shield, both in granite-greenstone and in granulite-facies terrains. All zircon crystals show complex internal structures, but magmatic and metamorphic ages are restricted to the Trans-Amazonian Cycle between 2228 Ma and 2051 Ma. The Trans-Amazonian Cycle is a dominantly juvenile event followed shortly thereafter by crustal recycling.

The Tandilia Belt exhibits a comparable petro-tectonic evolution to the Piedra Alta Terrane of Uruguay and to the basement of the Dom Feliciano Belt in southern Brazil. These results require a re-evaluation and integration of the models proposed for the evolution of the southern Brazilian shield in relation to western Gondwana and other Precambrian supercontinents. Although only one Archean age is registered in the dated zircon crystals, Nd isotopic data on 13 samples show that the Tandilia Belt has Neoproterozoic crust formation ages, similar to other rocks from the southern Brazilian shield.

## Introduction

THE TANDILIA BELT is the southernmost extension of the Brazilian shield in central Argentina, and is key to the understanding of its evolution. Geological relationships of the granites, gneisses, and migmatites in the belt are well understood, but absolute ages are only constrained by Rb-Sr and K-Ar geochronology. The interpreted time span of formation

of the belt is between 2.3 and 1.9 Ga, which requires re-evaluation based on zircon geochronology.

Precise dating of crustal accretion in the Rio de la Plata craton is also of major significance for the reconstruction of the geodynamic evolution of supercontinents during the Precambrian. We used the 30 µm spot analytical capability of the sensitive high-resolution ion microprobe (SHRIMP II) to determine the ages of magmatic crystallization and metamorphic recrystallization of zircon crystals from 10 rocks. These results are integrated with the geology and Sm-Nd isotopic geochemistry of 13

<sup>1</sup>Corresponding author; email: leo.hartmann@ufrgs.br

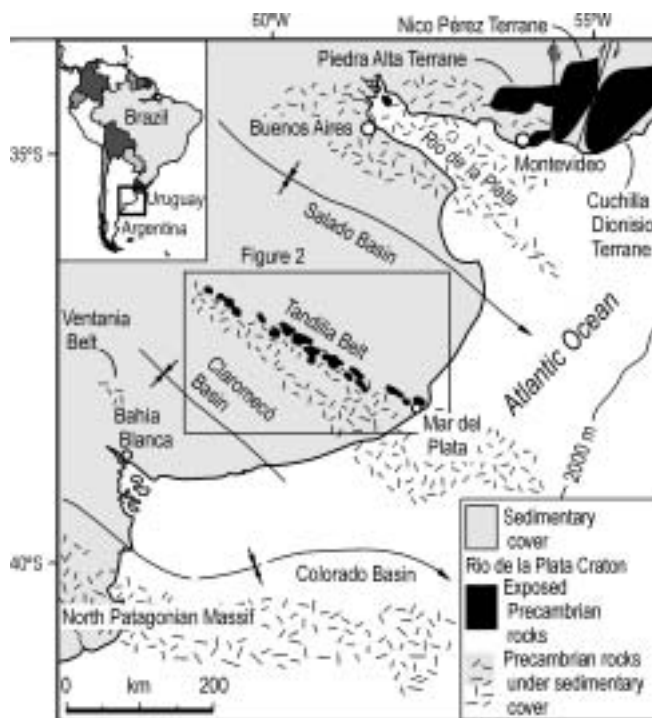


FIG. 1. Geological map of the southern portion of the Brazilian shield in Uruguay and eastern Argentina. Based on Ramos (1996).

rocks for the interpretation of the evolution of this Paleoproterozoic orogenic belt.

### Geological and Tectonic Setting

The Brazilian shield consists of three major cratons—the Amazon, São Francisco, and Rio de la Plata cratons, which are large segments of continental crust preserved from Neoproterozoic deformation (e.g., Brito Neves et al., 1999; Hartmann and Delgado, 2001; Hartmann, 2002). The southernmost extension of the Rio de la Plata craton crops out along western Uruguay (Piedra Alta and Nico Pérez terranes), in Martín García Island, and in the Tandilia Belt of Buenos Aires Province, Argentina (Fig. 1). Rocks and structures are rather varied in the Rio de la Plata craton, thus making it important to obtain accurate ages for the Tandilia Belt. In the Tandilia Belt, Precambrian basement forms a WNW-ESE granitic igneous-metamorphic belt—the Buenos Aires Complex (Marchese and Di Paola, 1975). Previous K-Ar and Rb-Sr geochronological data suggest a protracted geological evolution,

mainly within the Trans-Amazonian Cycle (Teruggi et al., 1973, 1974a; Teruggi and Kilmurray, 1980; Dalla Salda et al., 1988, 1992; Pankhurst et al., 2001).

The Buenos Aires Complex consists of granitic to tonalitic gneisses, migmatites, and amphibolites (Figs. 2 and 3), although rare schists, marbles, metavolcanics, and some acidic and basic mafic dikes are also present. Wide mylonitic zones are conspicuous. Low-grade metamorphic rocks occur in the Tandilia area, consisting of metacherts, meta-graywackes, and metabasites, interpreted as a slice of oceanic crust (Teruggi et al., 1988).

The metamorphic rocks of the Tandilia Belt are more voluminous in the Balcarce area, and include gneissic and migmatitic rocks, orthopyroxene-bearing granulites and a few schists, olivine marbles, and pyroxene-rich ultramafic lenses (Teruggi et al., 1974a; Cortelezzi et al., 1999). The main regional metamorphic event reached amphibolite facies and locally granulite facies, although many rocks are partly retrogressed to greenschist facies. In addition to the Balcarce area, a patch of mylonitized granu-

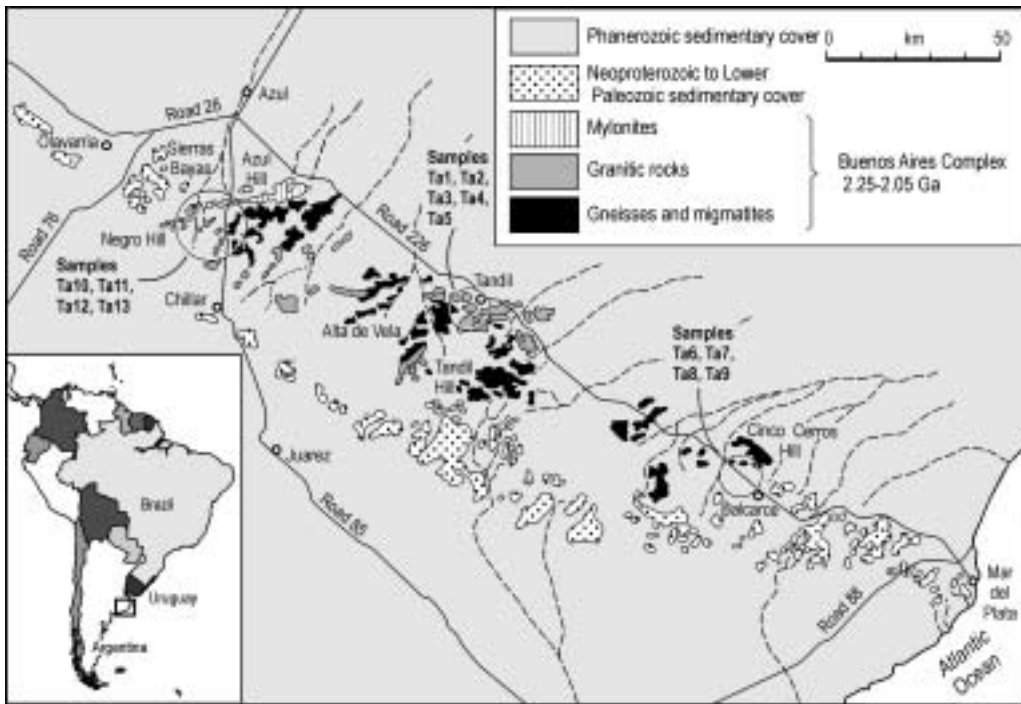


FIG. 2. Geological map of Tandilia Belt, eastern Argentina, showing the distribution of Buenos Aires Complex granites, gneisses, and migmatites. Based on Teruggi et al. (1973) and Iñiguez et al. (1989). Location of dated samples indicated; samples Ta2, Ta5, and Ta13 have whole-rock Sm-Nd isotopic determinations, the other 10 have additionally U-Pb zircon SHRIMP isotopic determinations.

litic rocks is also present in the Azul area. Plutonic rocks of granitic composition are dominant in the Tandilia Belt, but acidic metavolcanic rocks also occur south of the town of Tandil (Sierra de Vela and La Ribulia). Amphibole-bearing rocks are common in the Tandilia Belt, and are better represented in the southern and central regions.

A complex set of granitic plutons, gneisses, and migmatites characterizes the Buenos Aires Complex. Many of the plutons are deformed in the mylonite zones. Greenish gray granitoids (mainly tonalitic-granodioritic) are widespread in the complex, except in the northwestern area, where red monzogranitic rocks prevail—e.g., in the Sierra Chica and Sierras Bayas, near Olavarria. Whole-rock geochemistry (Dalla Salda et al., 1992) indicates the predominance of tonalites and granites in the Tandilia Belt, corresponding to three magmatic suites. One suite is tonalitic-trondhjemitic, another is high-K calc-alkaline, and the third is peraluminous S-type. This is interpreted as the result of

sequential evolution from an active continental margin to a continental collision. For instance, Pankhurst et al. (2001) considered the Buenos Aires Complex granitic rocks to be a metaluminous, I-type, formed at a convergent margin.

K-Ar and Rb-Sr data (with relatively low  $^{87}\text{Sr}/^{86}\text{Sr}$  initial ratios) indicate 2200–1900 Ma ages (Halpern and Linares, 1970; Teruggi et al., 1973, 1974a; Dalla Salda, 1981; Varela et al., 1988). The Sierra de Vela and Montecristo leucogranites (Tandil region) show younger Rb-Sr ages (1800–1600 Ma), with high  $^{87}\text{Sr}/^{86}\text{Sr}$  initial ratios (Varela et al., 1985; Dalla Salda et al., 1992). Recent Rb-Sr whole-rock isotopic data (Pankhurst et al., 2001) yield an isochron of  $1964 \pm 95$  Ma, within the same time range of previous investigations. A Sm-Nd isochron by Pankhurst et al. (2001) of  $\sim 2140 \pm 66$  Ma is considered the age of igneous precursors of the complex, whereas crust-derived Sm-Nd model ages of  $\sim 2620 \pm 80$  Ma indicate Neoproterozoic ages for the protolith of the granitic magmas.

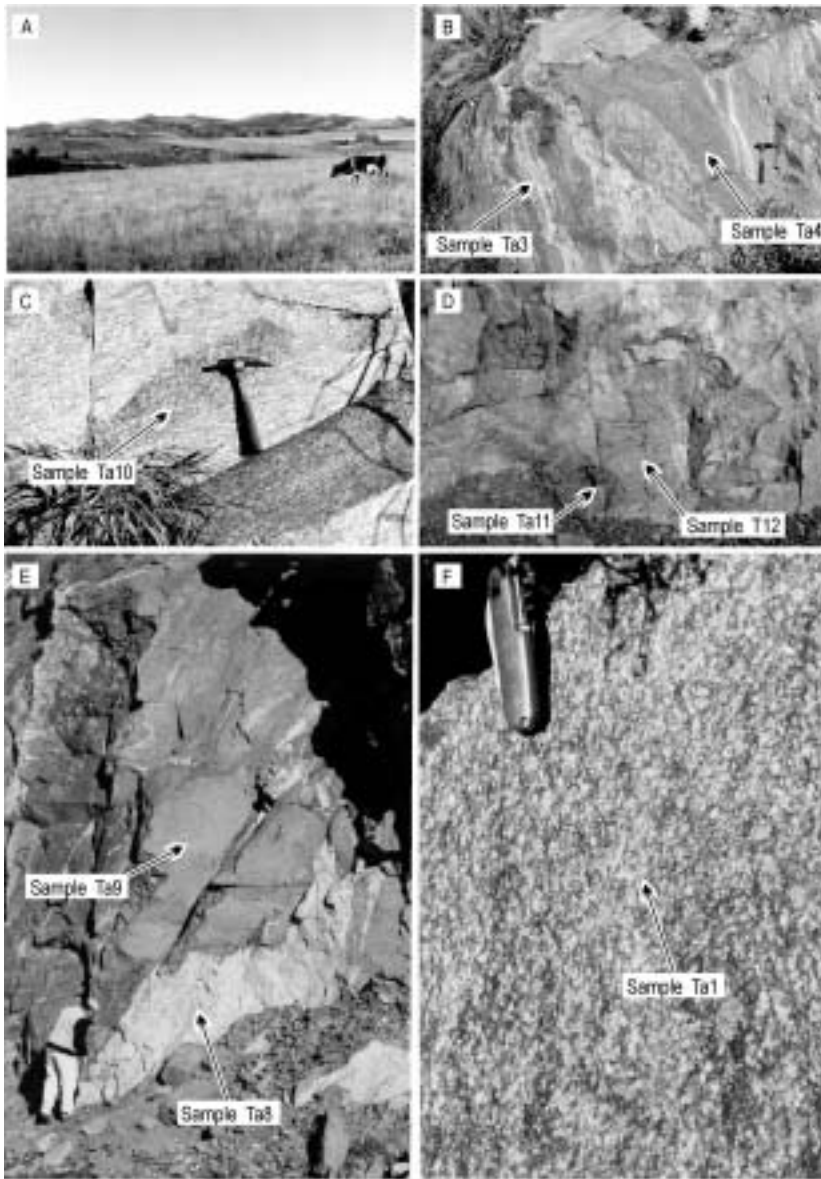


FIG. 3. Field photographs of the Tandilia Belt. A. Tandilia Hills as seen from the quarry, location of sample 1, at the foot of Calvário Hill. B. Roadcut on Route (Ruta) 30. C. Roadcut in Azul region. D. Villa Monica quarry, Azul region; charno-enderbite remnants in monzogranite. E. Punta Tota, Balcarce region. F. Roadcut, Azul region; subvertical mylonitic foliation.

The Buenos Aires Complex is intruded by a swarm of unmetamorphosed basic, intermediate, and acidic dikes (Teruggi et al., 1974b; Dalla Salda et al., 1988; Fernandez and Echeveste, 1995).  $^{40}\text{Ar}/^{39}\text{Ar}$  and K-Ar dating provided the distinction

between the calc-alkaline Paleoproterozoic (2020–2007 Ma) andesitic-basaltic, andesitic, and rhyolitic dikes and the tholeiitic Mesoproterozoic (1590 Ma) basaltic dikes (Iacumin et al., 2001; Teixeira et al., 2001).

TABLE 1. Description of Dated Rocks from the Buenos Aires Complex, Tandilia Belt

Sample number and rock type	Location, UTM coordinates	Description
Tandil region		
Ta1, Calvário Hill tonalite	Quarry behind communication tower, west of town of Tandil	Rocks show subvertical E-W foliation marked by 10–20 cm mafic schlieren. Thin, 10–30 cm thick shear zones occur, with epidote and quartz segregations. Rock sample is grey.
Ta2, diabase dike	37°21'0.18" S 59°10'0.44" W	Quarry behind a restaurant. Diabase is dark; plagioclase is greenish dark gray. Grain size about 0.5–2.0 mm. Rock is unfoliated.
Ta3, Ruta 30 tonalitic gneiss	37°22'0.33" S 59°12'0.21" W	Road cut about 10 km south of town of Tandil. Subvertical foliation, banding about 1–30 cm thick marked by dark and light gray gneisses. Small (20 cm) xenoliths of mafic rock present.
Ta4, Ruta 30 monzogranite	37°22'0.33" S 59°12'0.21" W	Massive, homogeneous, dark grey, 1–5 m thick intrusion into Ta3.
Ta5, Montecristo Hill trondhjemite	37°22'0.15" S 59°10'0.42" W	Quarry, SW of Tandil. Homogeneous, medium-grained, grey rock. No xenoliths of shear zones observed.
Balcarce region		
Ta6, Chacofi quarry mafic garnet gneiss	37°45'0.06" S 58°19'0.46" W	The mafic garnet gneiss is about 80 m thick. Rock is dark grey, medium grained; garnet crystals are red, 1 mm in size.
Ta7, Chacofi quarry garnet tonalite	37°45'0.06" S 58°19'0.46" W	Intrusive into Ta6-type rocks. Massive or in 1 m thick bands. Light grey.
Ta8, Punta Tota banded garnet gneiss	37°49'0.26" S 58°12'0.15" W	Dark grey; foliated.
Ta9, Cerro Triunfo mafic charnockitic gneiss	37°49'0.26" S 58°12'0.15" W	Mafic to intermediate orthopyroxene-bearing gneiss. Massive to banded rock. Some garnet present.
Azul region		
Ta10, road cut, syenogranite	37°13'0.53" S 59°45'0.24" W	Porphyritic rock. Feldspar phenocrysts are 1–2 cm large; matrix is dark grey about 0.2 mm. Magmatic flow marked by subvertical feldspar orientation. E-W shearing present; some rounding of feldspar by shearing. Some garnet formed during shearing. No garnet seen in undeformed granite 500 m from sample location.
Ta11, Villa Monica quarry grey charnoenderbite	36°54'0.42" S 60°08'0.45" W	Dominant rock in quarry. Unfoliated, greenish grey. Orthopyroxene identified in thin section.
Ta12, Villa Monica quarry red monzogranite	36°54'0.42" S 60°08'0.45" W	Intrusive into charno-enderbite, but mixture of two lithologies is very intense and present at all scales.
Ta13, La Tinta quartz sandstone	36°56'0.01" S 60°10'0.32" W	Sedimentary rock; basal unit of the group, directly over basement.

The tectonic evolution of the Buenos Aires Complex includes more than one deformational event (Teruggi et al., 1973, 1974a; Dalla Salda et al., 1988; Ramos, 1999; Cingolani and Dalla Salda, 2000) that produced complex interference patterns

within the geological units. The oldest major deformational event produced E-W-trending folds, commonly showing flat-lying limbs. These are most evident in the Tandil region. This event was succeeded by NE-trending open folds, also well dis-

TABLE 2. Sm-Nd Isotopic Data of Tandilia Belt Samples<sup>1</sup>

Sample	Sm , ppm	Nd , ppm	<sup>147</sup> Sm/ <sup>144</sup> Nd	<sup>143</sup> Nd/ <sup>144</sup> Nd	Error, ± σ	εNd (o)*	U-Pb age, Ma	εNd(t)	T <sub>DM</sub> , Ma
Ta1	5.067	28.852	0.1061	0.511177	70	-28.5	2234	-2.85	2668
Ta2	3.673	12.283	0.1807	0.51256	14	-1.49	1780*	1.8	2319
Ta3	5.0781	34.0758	0.090100	0.510999	23	-31.97	2183	-2.43	2538
Ta4	5.3685	36.7151	0.088400	0.511032	8	-31.32	2188	-1.23	2462
Ta5	15.97	92.155	0.1048	0.511472	58	-22.75	2100*	2.52	2155
Ta6	5.136	26.3084	0.118030	0.511454	7	-23.1	2194	-1.27	2558
Ta7	9.6613	52.9459	0.110320	0.511326	12	-25.59	2073	-2.95	2555
Ta8	20.832	107.45	0.1172	0.511357	14	-24.99	2176	-3.12	2693
Ta9	13.053	65.454	0.1205	0.511429	13	-23.59	2127	-3.12	2671
Ta10	14.3845	100.0587	0.086920	0.511053	9	-30.91	2109	-1.53	2407
Ta11	7.2686	39.8965	0.110150	0.511384	14	-24.46	2169	-0.69	2463
Ta12	4.8418	35.106	0.0834	0.510977	10	-32.4	2065	-2.71	2431
Ta13	2.563	11.688	0.1326	0.511718	9	-17.94	700*	-12.57	2523

<sup>1</sup>Explanatory notes: <sup>147</sup>Sm decay constant = 6.53974<sup>-12</sup>; <sup>147</sup>Sm/<sup>144</sup>Nd = 0.1967; \* = estimated age; <sup>143</sup>Nd/<sup>144</sup>Nd = 0.512638; <sup>143</sup>Nd /<sup>144</sup>Nd<sub>present</sub> = 0.512638 (<sup>146</sup>Nd/<sup>144</sup>Nd = 0.72190); εNd(0) = {(<sup>143</sup>Nd/<sup>144</sup>Nd [sample, measured value]/0,512638) × 10<sup>4</sup>}; εNd(t) = {(<sup>143</sup>Nd/<sup>144</sup>Nd [sample,t]-1) × 10<sup>4</sup>}; t = crystallization age.

played in the Tandil region. The third major event is NW trending. All three events are considered as remnants, after the strong superposition of a major subvertical, E-W-trending shear zone. The relative ages of these structures are evident on aerial photographs and outcrop exposures, but the absolute ages were only preliminarily determined as Paleoproterozoic, while it remains open whether the youngest structures were formed in the Neoproterozoic.

The Trans-Amazonian Cycle is interpreted as a continent-continent collisional event in the Tandilia Belt, as suggested by the injection of leucogranites, development of thick mylonite zones, ocean-floor rocks, and presumed thickening of the crust (Ramos, 1988, 1999; Teruggi et al., 1988; Dalla Salda et al., 1992). The collision caused thrusting and transcurrent faulting favoring anatexis of the crustal rocks. Furthermore, the emplacement of the granitoid plutons in the thick gneissic sequence in the Tandil area appears to be coeval with the regional high-temperature metamorphism, mylonitization, and anatexis. The leucogranites are heterogeneous, highly radiogenic, and typically post-collisional. The younger tholeiitic dikes constrain the timing of crustal extension following the last stages of mobile belt evolution in the Rio de la Plata craton (Teixeira et al., 1999). Finally, the Tandilia crust was variably affected by tectonothermal overprints, as shown by K-Ar whole-rock apparent ages between 980 and 790 Ma. The Buenos Aires Complex was partially covered by two platformal sedi-

mentary sequences, one during the Neoproterozoic and the other during the Early Paleozoic (Dalla Salda and Iñiguez, 1979; Iñiguez et al., 1989).

### Geochronology

The 10 rocks selected for zircon geochronology (13 for Sm-Nd isotopic geochemistry) are representative of the Buenos Aires Complex (Table 1). Minerals were separated in preparation for SHRIMP analyses by grinding crushed samples in a ring mill to pass through a 60 # nylon disposable sieve, washing and decanting fines with water, and then heavy liquid (LST and di-iodomethane), and magnetic separation before hand-picking representative grains using a binocular microscope. Selected grains were mounted on an epoxy disc with chips of the Perth CZ3 zircon standard, ground and polished until nearly half of each grain was removed, microphotographed in transmitted and reflected light, and imaged for their internal morphology using a scanning electron microscope (i.e., backscattered electrons). The mount was then cleaned and gold-coated in preparation for SHRIMP analyses. The isotopic composition of the zircons was determined using SHRIMP II (e.g., De Laeter and Kennedy, 1998) installed at Curtin University of Technology, Perth Australia using methods originally published by Compston et al. (1992) and more recently stated by Smith et al. (1998). The uncertainty in all pooled ages is at the 95% confidence level. SHRIMP isotopic data were

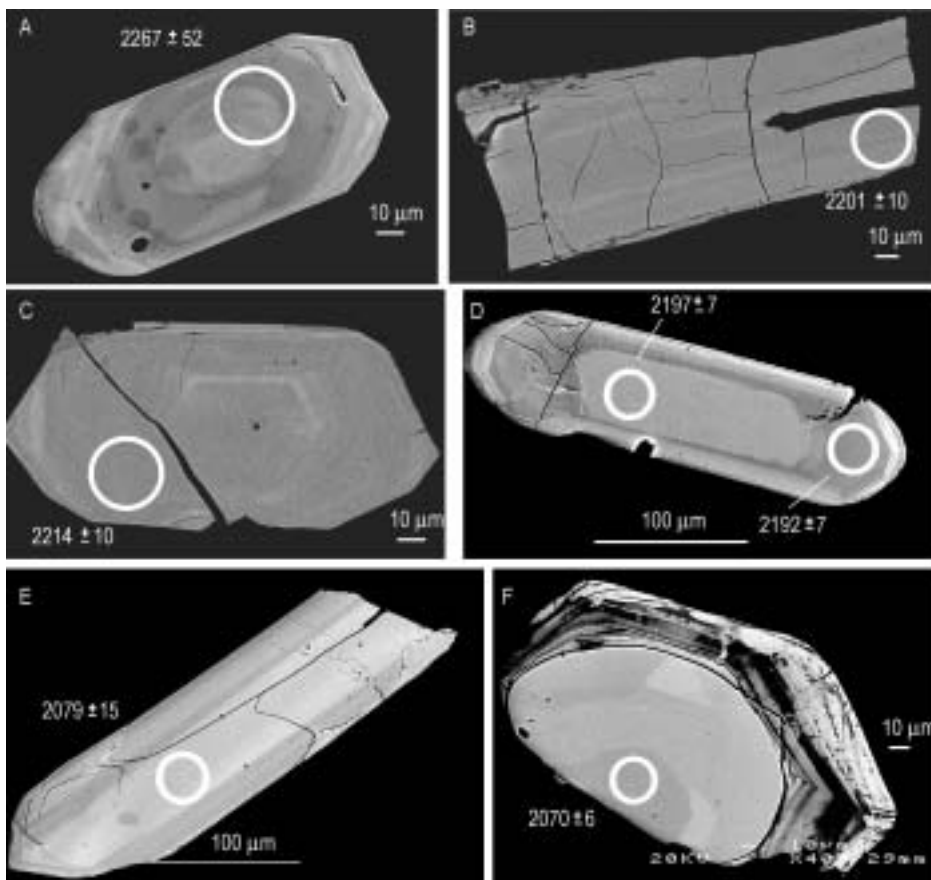


FIG. 4. Backscattered electron images of analyzed zircon crystals. A. Sample Ta1. B. Sample Ta3. C. Sample Ta4. D. Sample Ta6. E and F. Sample Ta7. Location of analyzed spot indicated by circle and age obtained shown in Ma.

reduced with the use of the software Isoplot/Ex (Ludwig, 1999) and Squid 1.02 (Ludwig, 2001).

Sm-Nd isotopic determinations were made on 13 rock samples at the geochronology laboratory of Universidade de Brasília, Brazil (Table 2). Most of the rocks were derived from Archean crust, as indicated by the Sm-Nd model  $T_{DM}$  ages (DePaolo, 1988) in the 2668–2440 Ma range (samples Ta1, Ta3, Ta4, Ta6, Ta7, Ta9, and Ta13). The  $\epsilon Nd$  values slightly below zero (–1.27 to –3.30) are another argument for a crustal source for most of the granitoids, but this crustal source cannot be much older than the magmatism because the values are small. However, the Montecristo leucogranite (Ta5) has a younger model age (2215 Ma) and is interpreted as derived from a Paleoproterozoic source. This rock was not dated by zircon U-Pb isotopes, but if we

consider its magmatic age as bracketed between the older granitoids, such as Ta1, and the younger granitoids, such as Ta12, then the  $\epsilon Nd$  of sample Ta5 is between +2.95 and +1.23. Therefore, the Montecristo leucogranite is more closely related to the Trans-Amazonian mantle than all other investigated samples. The  $\epsilon Nd$  values (Table 2) for the Ta2 mafic dike (+1.80) and for the Ta13 younger quartzite (–8.46) were calculated assuming, respectively, the ages of 1780 Ma (intrusion age) and 1200 Ma (metamorphic age).

The complex internal structure observed in BSE images in most zircon crystals from 10 rock samples (Figs. 4 and 5; zircon description in Appendix A) seem to have formed mostly within the time span of the Trans-Amazonian Cycle. The SHRIMP U-Pb weighted mean  $^{207}Pb/^{206}Pb$  ages obtained from 10

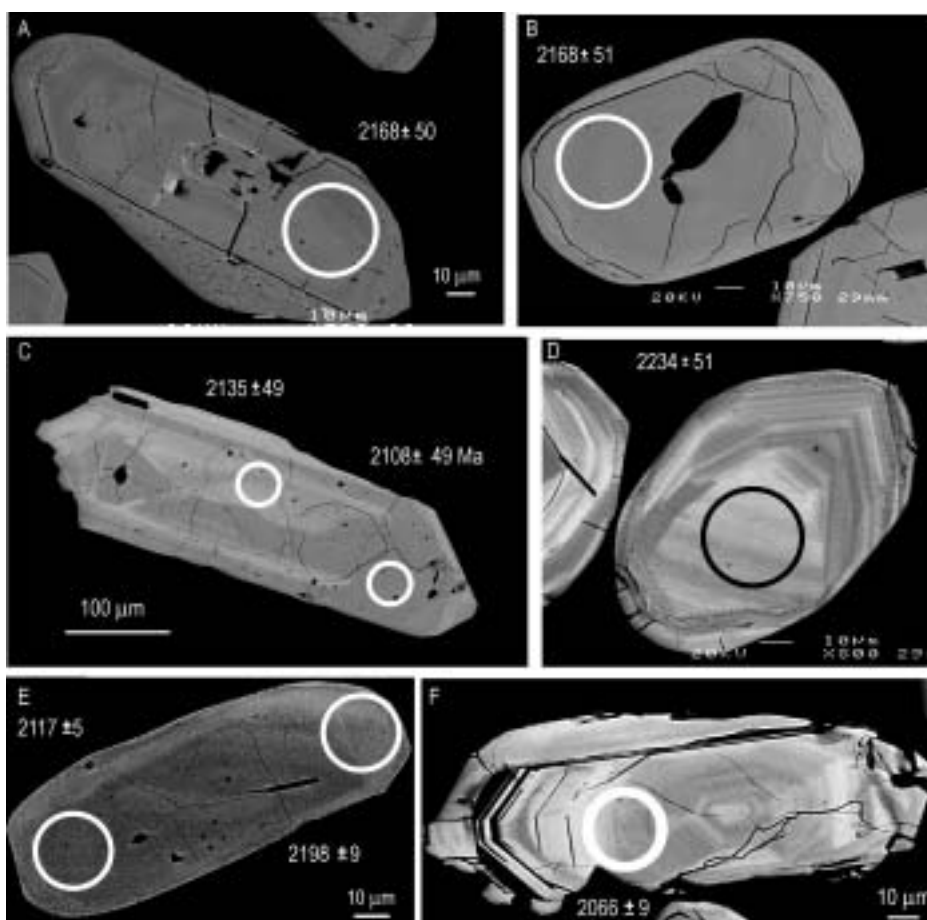


FIG. 5. Backscattered electron images of analyzed zircon crystals. A and B. For Sample Ta8. C. Sample Ta10; D. sample Ta11. E. Sample Ta9. F. Sample Ta12. The location of the analyzed spot is indicated by the circle and the age obtained is shown in Ma.

rock samples (62 zircon crystals) are in the 2228–2051 Ma range (Figs. 6 and 7; Table 3). The oldest rock is the Tandil tonalite (Ta1), which crystallized at  $2228 \pm 6$  Ma, and the youngest rock is the Azul red granite, Ta12 ( $2051 \pm 3$  Ma). Another young rock is the Balcarce tonalite Ta7,  $2073 \pm 6$  Ma. Rocks with intermediate ages are found in all domains of the Tandilia Belt, such as samples Ta4 of Tandil ( $2166 \pm 7$  Ma), Ta8 of Balcarce ( $2163 \pm 8$  Ma), and Ta11 of Azul ( $2162 \pm 5$  Ma). The concentration of ages in two maxima near 2.16 Ga and 2.08 Ga (Fig. 8) has been found in many occurrences of Paleoproterozoic rocks in South America, and is

commonly ascribed to the accretionary Encantadas orogeny and the collisional Camboriú orogeny of the Trans-Amazonian Cycle.

Inherited zircon crystals are present in most samples and their ages are dominantly Paleoproterozoic, slightly older than the magmatic age of the zircon crystals (Table 3). Despite the strong indication obtained from Nd isotopic geochemistry for a Neoproterozoic age of the source of most samples, only the Tandil tonalite gneiss (Ta3) revealed an Archean zircon age after SHRIMP dating, and this is slightly older (2657 Ma) than the Nd model age (2515 Ma) of the same sample.



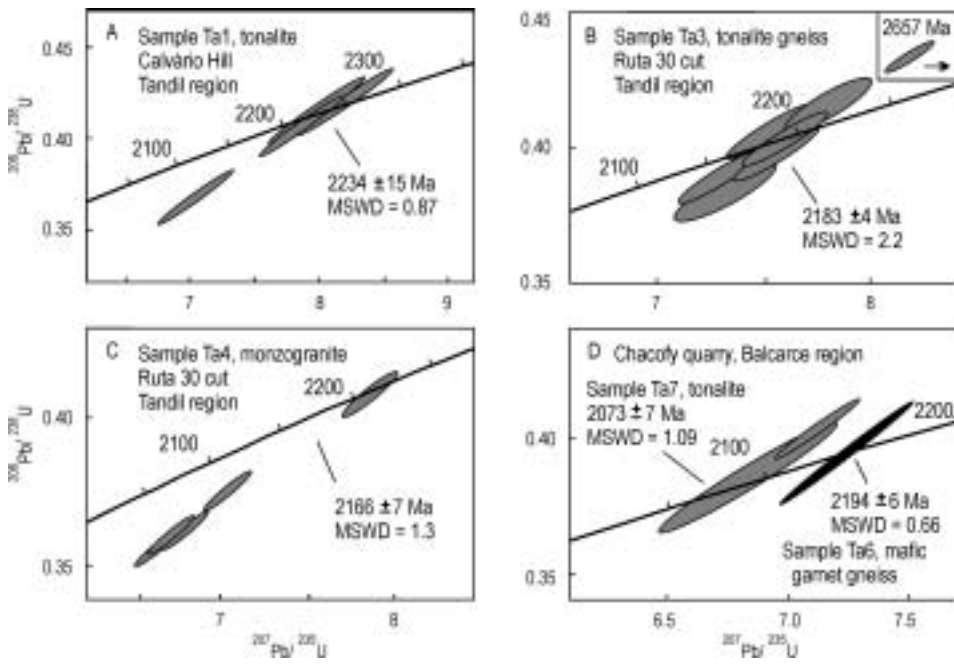


FIG. 6. Concordia diagrams of samples Ta1, Ta3, Ta4, Ta6, and Ta7.

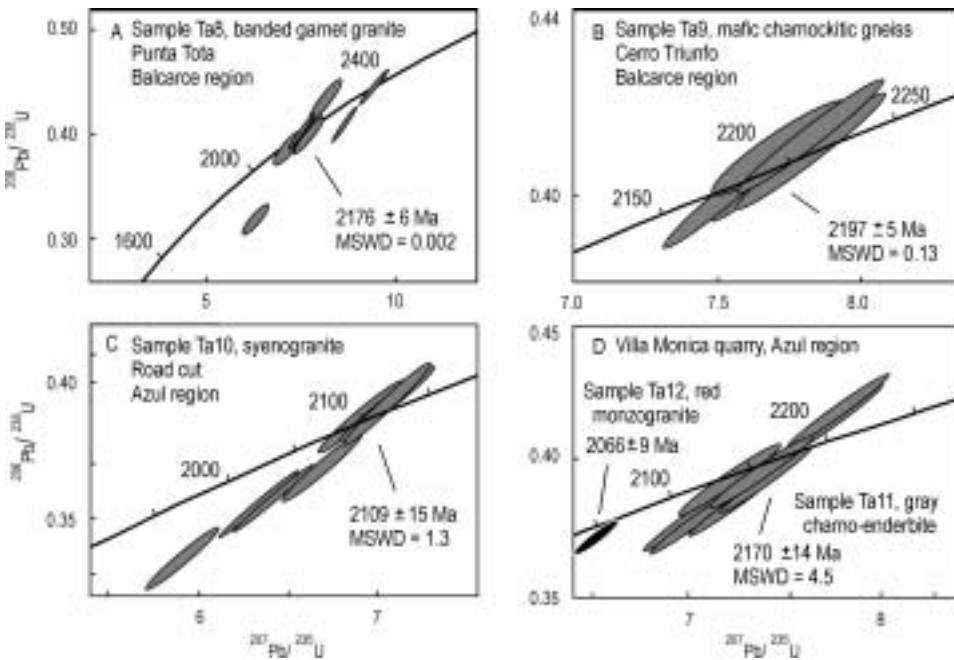


FIG. 7. Concordia diagrams of samples Ta8, Ta9, Ta10, Ta11, and Ta12.

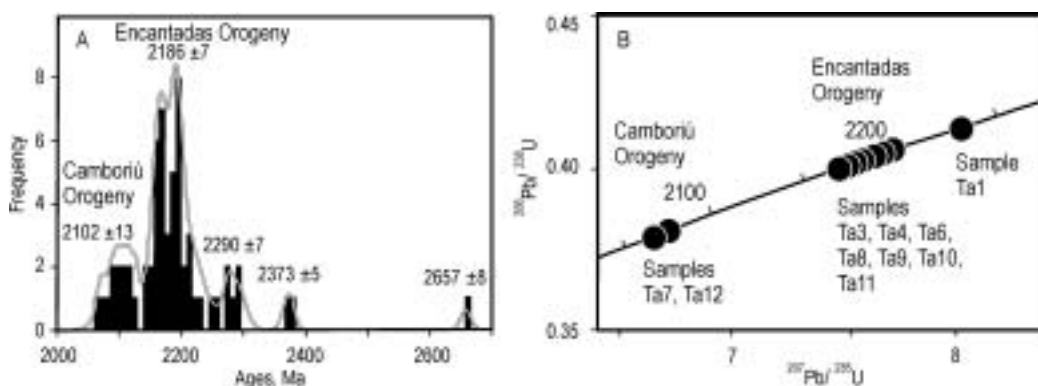


FIG. 8. A. Frequency histogram of 62 weighted mean  $^{207}\text{Pb}/^{206}\text{Pb}$  zircon ages from the Buenos Aires Complex, Tandilia Belt, zircon crystals analyzed in this investigation. The bimodal distribution of ages is due to the formation and deformation of rocks during the Encantadas and Camboriú orogenies in this Trans-Amazonian Cycle belt. B. Model concordia diagram showing interpreted ages of magmatic and metamorphic events from the 10 analyzed rocks. The isotopic imprint of the two orogenies of the Trans-Amazonian Cycle is evident.

### Concluding Remarks

Reliable ages for gneissic and granitoid rocks have been determined in the Tandilia Belt for the first time in this investigation using the robust zircon U-Pb SHRIMP isotopic technique—61 analyses in 56 zircon crystals from 10 rock samples. Regardless of composition and structure, the magmatic ages of all units are Paleoproterozoic (Riarian) in the range 2228–2051 Ma. Age of inheritance determined in the cores of a few zircon crystals suggest 2371 (Siderian) to 2135 Ma (Early Riarian) for the source, with only one Neoproterozoic age of ~2657 Ma in a tonalite from the Tandil region. Complex internal structures of zircon crystals seen on backscattered electron images are suggestive of metamorphic recrystallization, but the ages are all within the error of the magmatic ages, indicating that the deformation (including mylonitization) occurred shortly after the magmatic crystallization, entirely within the Trans-Amazonian Cycle. The lack of recrystallization or new zircon growth in the Neoproterozoic suggests that the Tandilia Belt was little affected by younger orogenies such as those of the Brasiliano Cycle, although less intense deformation may have occurred and remained unregistered in the zircons.

These data confirm previous interpretations that the Buenos Aires Complex was formed during the Trans-Amazonian Cycle (2.25–2.0 Ga) in the Tandilia Belt. It is important to note that the Sm-Nd

$T_{\text{DM}}$  model ages, representing the ages of the protoliths, vary from 2668 to 2319 Ma, comparable to the  $2620 \pm 80$  Ma model age obtained by Pankhurst et al. (2001). The tectonic scenario seems related to juvenile accretion along an active continental margin, followed by continental collision. The Paleoproterozoic collision may have involved an older continent such as the Nico Pérez Terrane of Uruguay, which is known to contain Archean terrains (Hartmann et al., 2001).

The rock formation age at ~2150 Ma is dominant in the total age range 2228–2051 Ma found in the Tandilia Belt. This 2150 Ma age is recognized in South America as a major accretionary orogenic event, the Encantadas orogeny, covering the time range of 2.25–2.10 Ga (e.g., Hartmann and Delgado, 2001). Extensive granite-greenstone belt terrains formed at ~2.15 Ga in Guyana, French Guiana, Suriname, and extending into Brazil in Amapá and including Bahia state. In the southern Brazilian shield, a similar age of ~2.15 Ga was found in the Paso Severino greenstone belt north of Montevideo in the core of the Rio de la Plata craton. The Tandilia Belt is equivalent to a deeper crustal level, plutonic environment of the Piedra Alta Terrane, which contains the Paso Severino greenstone belt in Uruguay.

The youngest age peak at ~2.08 Ga is the dominant age of granulite-facies deformation of rocks in South America during the collisional Camboriú orogeny (Hartmann and Delgado, 2001), including

TABLE 3. SHRIMP Zircon U-Pb Isotopic Data of Buenos Aires Complex, Tandilia Belt<sup>1</sup>

Spot	U, ppm	Th, ppm	Th, U	4f206 (%)	Isotopic ratios				Ages		Disc %	
					207/206	208/206	206/238	207/235	207/206	206/238		
Sample Ta1, Calvarío hill tonalite, Tandil region												
a.2-1	82	39	0.50	-0.03	0.1442 ± 1.02	0.1399 ± 1.10	0.4131 ± 2.80	8.2137 ± 2.98	0.1174 ± 3.61	2278 ± 18	2229 ± 53	2
a.4-1	90	45	0.52	-0.13	0.1447 ± 0.99	0.1484 ± 1.03	0.4059 ± 2.78	8.0970 ± 2.95	0.1178 ± 3.10	2284 ± 17	2196 ± 52	4
a.5-1	339	105	0.32	0.41	0.1391 ± 0.61	0.1068 ± 0.65	0.3672 ± 2.68	7.0426 ± 2.75	0.1123 ± 3.37	2216 ± 11	2016 ± 46	9
a.10-1	173	152	0.91	-0.01	0.1415 ± 0.65	0.2603 ± 0.80	0.4214 ± 2.71	8.2218 ± 2.79	0.1208 ± 2.90	2246 ± 11	2267 ± 52	-1
a.12-1	89	77	0.89	0.04	0.1395 ± 0.67	0.2499 ± 0.80	0.4155 ± 2.77	7.9933 ± 2.85	0.1168 ± 2.89	2221 ± 12	2240 ± 52	-1
a.16-1	306	88	0.30	0.07	0.1403 ± 0.46	0.0835 ± 0.89	0.4068 ± 2.71	7.8687 ± 2.75	0.1124 ± 3.01	2231 ± 8	2200 ± 51	1
Sample Ta3, Ruta 30 tonalitic gneiss, Tandil region												
a.4-1	77	31	0.41	-0.01	0.1379 ± 0.58	0.1192 ± 0.96	0.3978 ± 1.59	7.5635 ± 1.69	0.1161 ± 1.89	2201 ± 10	2159 ± 29	2
a.6-1	30	10	0.33	-0.02	0.1385 ± 1.00	0.0995 ± 1.81	0.3837 ± 1.87	7.3258 ± 2.12	0.1169 ± 3.10	2208 ± 17	2094 ± 33	5
a.14-1	152	69	0.47	0.05	0.1804 ± 0.46	0.1330 ± 1.44	0.4734 ± 1.49	11.7766 ± 1.56	0.1347 ± 2.34	2637 ± 8	2498 ± 31	6
a.15-1	73	61	0.86	0.11	0.1361 ± 0.63	0.2474 ± 0.75	0.3889 ± 1.61	7.2962 ± 1.73	0.1122 ± 1.81	2178 ± 11	2118 ± 29	3
a.16-1	55	18	0.35	0.11	0.1350 ± 0.80	0.0965 ± 1.26	0.4062 ± 1.67	7.5609 ± 1.86	0.1137 ± 2.34	2164 ± 14	2198 ± 31	-2
a.17-1	67	59	0.90	0.09	0.1365 ± 0.78	0.2574 ± 0.75	0.4044 ± 1.62	7.6102 ± 1.80	0.1156 ± 1.82	2183 ± 14	2189 ± 30	0
a.18-1	59	32	0.56	0.13	0.1362 ± 0.79	0.1583 ± 0.98	0.4153 ± 1.66	7.7968 ± 1.84	0.1177 ± 2.08	2179 ± 14	2239 ± 31	-3
a.19-1	324	220	0.70	0.02	0.1367 ± 0.36	0.1980 ± 0.42	0.4005 ± 1.46	7.5462 ± 1.50	0.1133 ± 1.52	2185 ± 6	2171 ± 27	1
a.20-1	339	351	1.07	0.04	0.1367 ± 0.44	0.3003 ± 3.23	0.4041 ± 1.46	7.6167 ± 1.53	0.1136 ± 4.42	2186 ± 8	2188 ± 27	0
Sample Ta4, Ruta 30 monzogranite, Tandil region												
d.2-1	284	195	0.71	0.20	0.1346 ± 0.39	0.2065 ± 0.42	0.3606 ± 1.46	6.6936 ± 1.51	0.1052 ± 1.53	2159 ± 7	1985 ± 25	8
d.3-1	203	145	0.74	0.00	0.1354 ± 0.39	0.2058 ± 1.47	0.3754 ± 1.48	7.0083 ± 1.53	0.1048 ± 2.83	2169 ± 7	2055 ± 26	5
d.4-1	198	18	0.10	0.15	0.1347 ± 0.48	0.0337 ± 9.43	0.3562 ± 1.49	6.6143 ± 1.56	0.1256 ± 11.3	2160 ± 8	1964 ± 25	9
d.5-1	95	43	0.47	-0.04	0.1389 ± 0.60	0.1313 ± 0.84	0.4081 ± 1.56	7.8172 ± 1.67	0.1151 ± 1.80	2214 ± 10	2206 ± 29	0
d.7-1	275	178	0.67	0.06	0.1356 ± 0.36	0.1876 ± 0.84	0.3623 ± 1.48	6.7743 ± 1.52	0.1017 ± 1.96	2172 ± 6	1993 ± 25	8
d.11-1	160	177	1.14	0.05	0.1440 ± 0.43	0.3177 ± 0.45	0.4306 ± 1.51	8.5473 ± 1.57	0.1196 ± 1.59	2275 ± 7	2308 ± 29	-1
d.11-2	59	35	0.62	-0.01	0.1453 ± 0.67	0.1770 ± 0.96	0.4251 ± 1.65	8.5151 ± 1.78	0.1210 ± 1.95	2291 ± 12	2284 ± 32	0
Sample Ta6, Chacofi quarry mafic gneiss, Balcarce region												
b.1-1	589	1367	2.40	0.00	0.1377 ± 0.41	0.1723 ± 0.92	2.3538 ± 2.01	44.6849 ± 2.05	0.1690 ± 2.37	2198 ± 7	1801 ± 91	-255
b.1-2	167	95	0.59	-0.02	0.1373 ± 0.40	0.1690 ± 0.64	0.4119 ± 1.95	7.7971 ± 1.99	0.1181 ± 2.07	2193 ± 7	2224 ± 37	-1
b.10-1	209	121	0.60	-0.02	0.1375 ± 0.37	0.1729 ± 0.51	0.3821 ± 1.94	7.2470 ± 1.98	0.1099 ± 2.05	2196 ± 6	2086 ± 35	5
Sample Ta7, Chacofi quarry tonalite, Balcarce region												
k.1-1	72	25	0.36	0.03	0.1288 ± 0.79	0.1054 ± 1.06	0.3836 ± 2.04	6.8124 ± 2.19	0.1115 ± 2.34	2082 ± 14	2093 ± 37	-1
k.2-1	281	197	0.72	-0.02	0.1280 ± 0.37	0.2131 ± 1.58	0.3911 ± 2.09	6.9034 ± 2.12	0.1151 ± 2.81	2071 ± 6	2128 ± 38	-3

Sample Ta8, Punta Tota banded garnet granite, Balcarce region									
c.1-1	129	0.1373 ± 0.55	0.1201 ± 0.92	0.4062 ± 2.73	7.6916 ± 2.79	0.1170 ± 2.92	2194 ± 10	2198 ± 51	0
c.2-1	142	0.1335 ± 1.77	0.1437 ± 5.72	0.3856 ± 2.73	7.0971 ± 3.25	0.1133 ± 7.93	2144 ± 31	2102 ± 49	2
c.7-1	63	0.1383 ± 1.48	0.2536 ± 0.94	0.3997 ± 2.84	7.6197 ± 3.20	0.1236 ± 3.01	2206 ± 26	2168 ± 52	2
c.8-1	171	0.1528 ± 0.43	0.3115 ± 1.36	0.4443 ± 2.71	9.3577 ± 2.74	0.1263 ± 3.33	2377 ± 7	2370 ± 54	0
c.11-1	171	0.1520 ± 0.46	0.1450 ± 0.77	0.4081 ± 2.72	8.5525 ± 2.75	0.1143 ± 2.84	2368 ± 8	2206 ± 51	7
c.14-1	195	0.1349 ± 0.57	0.1023 ± 0.80	0.3999 ± 2.70	7.4736 ± 2.76	0.1158 ± 2.83	2163 ± 10	2168 ± 50	0
c.16-1	83	0.1356 ± 0.73	0.1137 ± 1.18	0.3999 ± 2.78	7.4743 ± 2.87	0.1150 ± 3.06	2171 ± 13	2168 ± 51	0
c.17-1	27	0.1353 ± 1.48	0.1490 ± 1.80	0.4331 ± 3.05	8.0783 ± 3.39	0.1235 ± 3.62	2320 ± 26	2320 ± 59	-7
c.19-1	75	0.1425 ± 1.60	0.1344 ± 2.18	0.3180 ± 2.87	6.2459 ± 3.29	0.1135 ± 3.73	2257 ± 28	1780 ± 45	21
Sample Ta9, Cerro Triunfo mafic charnockitic gneiss, Balcarce region									
b.3-1	321	0.1322 ± 0.31	0.0772 ± 3.08	0.3888 ± 2.07	7.0842 ± 2.09	0.1189 ± 4.14	2127 ± 5	2117 ± 37	7
b.3-2	133	0.1377 ± 0.52	0.1316 ± 0.72	0.4130 ± 1.91	7.8400 ± 1.98	0.1175 ± 2.06	2198 ± 9	2229 ± 36	0
b.4-1	114	0.1372 ± 1.21	0.1210 ± 0.81	0.4084 ± 1.95	7.7289 ± 2.29	0.1156 ± 2.13	2193 ± 21	2208 ± 36	0
b.5-1	178	0.1376 ± 0.39	0.1587 ± 0.56	0.4056 ± 1.78	7.6950 ± 1.82	0.1178 ± 1.97	2197 ± 7	2195 ± 33	0
b.6-1	178	0.1342 ± 0.74	0.1321 ± 1.48	0.3158 ± 1.78	5.8430 ± 1.93	0.1276 ± 2.90	2153 ± 13	1769 ± 28	1
b.7-1	167	0.1367 ± 0.46	0.1467 ± 0.65	0.4005 ± 1.99	7.5486 ± 2.04	0.1158 ± 2.14	2186 ± 8	2172 ± 37	2
b.8-1	98	0.1339 ± 0.88	0.1106 ± 0.98	0.3936 ± 2.13	7.2698 ± 2.31	0.1125 ± 2.37	2150 ± 15	2140 ± 39	0
b.12-1	155	0.1386 ± 0.50	0.1712 ± 0.58	0.4101 ± 1.89	7.8377 ± 1.96	0.1174 ± 2.00	2210 ± 9	2215 ± 36	21
Sample Ta10, Road cut syenogranite, Azul region									
d.1-1	208	0.1308 ± 0.47	0.2122 ± 0.56	0.3927 ± 2.70	7.0834 ± 2.74	0.1103 ± 2.77	2109 ± 8	2135 ± 49	-1
d.1-2	121	0.1292 ± 0.65	0.1557 ± 0.88	0.3869 ± 2.74	6.8947 ± 2.82	0.1118 ± 2.92	2088 ± 11	2108 ± 49	-1
d.3-1	384	0.1301 ± 0.54	0.1131 ± 0.57	0.3582 ± 2.68	6.4227 ± 2.73	0.1053 ± 3.14	2099 ± 9	1973 ± 45	6
d.4-1	82	0.1308 ± 0.87	0.2388 ± 0.89	0.3887 ± 2.79	7.0100 ± 2.92	0.1113 ± 2.93	2109 ± 15	2117 ± 50	0
d.5-1	337	0.1277 ± 0.76	0.0688 ± 2.05	0.3352 ± 2.69	5.9020 ± 2.79	0.0886 ± 4.42	2067 ± 13	1864 ± 44	10
d.10-1	330	0.1302 ± 0.43	0.1142 ± 0.70	0.3580 ± 2.69	6.4247 ± 2.72	0.1026 ± 2.80	2100 ± 7	1972 ± 46	6
d.11-1	441	0.1313 ± 0.34	0.1216 ± 0.52	0.3766 ± 2.67	6.8174 ± 2.69	0.1083 ± 2.74	2116 ± 6	2060 ± 47	3
d.14-1	191	0.1315 ± 0.52	0.1567 ± 0.74	0.3687 ± 2.71	6.6833 ± 2.76	0.1074 ± 2.81	2118 ± 9	2023 ± 47	4
d.16-1	355	0.1292 ± 0.39	0.1076 ± 0.66	0.3545 ± 2.68	6.3174 ± 2.71	0.1060 ± 2.78	2088 ± 7	1956 ± 45	6
Sample Ta11, Villa Monica quarry gray charmo-enderbite, Azul region									
e.5-1	274	0.1370 ± 0.43	0.1164 ± 0.70	0.3834 ± 2.69	7.2404 ± 2.73	0.1082 ± 2.79	2189 ± 7	2092 ± 48	4
e.6-1	162	0.1352 ± 0.72	0.1862 ± 0.74	0.3767 ± 2.73	7.0405 ± 2.82	0.1084 ± 2.84	2167 ± 13	2065 ± 48	5
e.7-1	129	0.1354 ± 0.67	0.0862 ± 1.24	0.3965 ± 2.76	7.4034 ± 2.84	0.1115 ± 3.06	2170 ± 12	2153 ± 50	1
e.9-1	254	0.1347 ± 0.49	0.1465 ± 0.67	0.3776 ± 2.71	7.0107 ± 2.76	0.1052 ± 2.81	2160 ± 9	2065 ± 48	4
e.12-1	153	0.1354 ± 0.54	0.1774 ± 0.72	0.4141 ± 2.72	7.7341 ± 2.78	0.1173 ± 2.83	2170 ± 9	2234 ± 51	-3
e.14-1	178	0.1350 ± 0.52	0.1869 ± 0.65	0.4182 ± 2.71	7.7810 ± 2.76	0.1208 ± 2.80	2163 ± 9	2252 ± 52	-4
e.19-1	194	0.1367 ± 0.49	0.1610 ± 1.14	0.3916 ± 2.71	7.3795 ± 2.76	0.1148 ± 2.99	2186 ± 9	2130 ± 49	3
e.19-2	75	0.1385 ± 0.78	0.1120 ± 1.30	0.3921 ± 2.80	7.2144 ± 2.91	0.1098 ± 3.12	2144 ± 14	2132 ± 51	1
Sample Ta12, Villa Monica quarry red monzogranite, Azul region									
l.2-1	255	0.1274 ± 0.55	0.1316 ± 0.76	0.3671 ± 1.69	6.4081 ± 1.77	0.1048 ± 1.87	2066 ± 9	2016 ± 29	2

<sup>1</sup>Isotopic ratios errors are in percent; all Pb in ratios are radiogenic component after correction for <sup>204</sup>Pb; disc. = discordance, as 100 - 100[(<sup>206</sup>Pb/<sup>238</sup>U)<sup>t</sup>/<sup>207</sup>Pb]<sub>i</sub>]; #206 = (common <sup>206</sup>Pb) / (total measured <sup>206</sup>Pb) or <sup>208</sup>Pb; Uncertainties are 1σ; disc. = discordance.

southern Brazil (Hartmann et al., 2000a). It is also an age of granite formation in shallower crustal levels, such as the Isla Mala granite in the Piedra Alta Terrane (Hartmann et al., 2000b) or the Arroio dos Ratos K-rich granite in southern Brazil (Leite et al., 2000). This indicates that the crust of the southern Brazilian shield, including the Tandilia Belt, was generated during two major orogenic events, the Encantadas orogeny 2.25–2.12 Ga and the Cambriú orogeny 2.10–2.00 Ga. The extent of Archean crust is rather limited (Hartmann et al., 2000a).

The Tandilia Belt is confirmed as the southernmost extension of the Rio de la Plata craton because of the ages within the Trans-Amazonian Cycle, and was formed by successive events within this cycle. This geological evolution can be correlated with the Piedra Alta Terrane (Uruguay), where Nd isotopic data and zircon SHRIMP U-Pb ages show a similar signature (Cingolani et al., 1997; Preciozzi et al., 1999; Hartmann et al., 2000b; Cingolani et al., 2001).

A new accurate time marker of 2228–2051 Ma is established here for the Tandilia Belt, a key area of southern South America, constraining more tightly the complex geotectonic evolution of the Paleoproterozoic Trans-Amazonian Cycle. The crustal residence time of the recycled crust was ~300 m.y., because the Trans-Amazonian cycle of orogenies involved Paleoproterozoic melting and deformation of Neoproterozoic rocks.

### Acknowledgments

This work was financed by project of excellence on “Geochemistry and Crustal Evolution of Southern South America,” Conselho Nacional do Desenvolvimento Científico e Tecnológico–Universidade Federale do Rio Grande do Sul (CNPq-FRGS), Brazil and supported by (Condejo Nacional de Investigaciones Científicas y Tecnológicas (CONICET), Argentina. SHRIMP II operations are headquartered at Curtin University of Technology, Perth, Western Australia, jointly with the University of Western Australia and the Geological Survey of Western Australia, with the support of the Australian Research Council. Access to SHRIMP was gained through collaboration with the Center for Global Metallogeny, University of Western Australia. We thank M. E. Teruggi and L. H. Dalla Salda for helpful revisions and comments. Paul Potter is acknowledged for a review of the English exposition.

### REFERENCES

- Brito, Neves, B. B., Campos Neto, M. C., and Fuck, R., From Rodinia to western Gondwana: An Approach to the Brasiliano–Pan African cycle and orogenic collage: Episodes, v. 22, p. 55–166.
- Cingolani, C., Bossi, J., Varela, R., Maldonado, S., Piñeyro, D., and Schipilov, A., 2001, Piedra Alta Terrane of Uruguay: Rb–Sr Geochronological data of two new Paleoproterozoic (Transamazonian) granitoids. III South American Symposium on Isotope Geology, Pucon, Chile, p. 109–112.
- Cingolani, C. A., and Dalla Salda, L. H., 2000, Buenos Aires cratonic region, *in* Cordani, U. G., Milani, E., Thomaz Filho, A., and Campos, D. A., eds., Tectonic evolution of South America: 31<sup>st</sup> International Geological Congress, Rio de Janeiro, p. 139–146.
- Cingolani, C. A., Varela, R., Dalla Salda, L., Bossi, J., Campal, N., Ferrando, L., Piñeyro, D., and Schipilov, A., 1997, Rb–Sr geochronology from the Rio de la Plata craton of Uruguay [abs.]: South American Symposium on Isotope Geology, Brazil, extended abstracts, p. 73–75.
- Compston, W., Williams, I. S., Kirschvink, J. L., Zichao, Zh., and Guogan, M., 1992, Zircon ages for the Early Cambrian time-scale: Journal of the Geological Society of London, v. 149, p. 171–184.
- Corteleszi, C. R., Ribot, A. M., and De Barrio, R. E., 1999, Los gneisses piroxénicos del basamento precámbrico de las Sierras de Balcarce, Tandilia, Argentina: XIV Congreso Geológico Argentino, Salta, Actas, v. II, p. 90–91.
- Dalla Salda, L., 1981, Tandilia, un ejemplo de tectónica de transcurrencia en basamento: Revista de la Asociación Geológica Argentina, v. 36, p. 204–207.
- Dalla Salda, L. H., Bossi, J., and Cingolani, C.A., 1988, The Rio de la Plata cratonic region of Southwestern Gondwanaland: Episodes, v. 11, no. 4, p. 263–269.
- Dalla Salda, L., Franzese, J., and Posadas, V.B., 1992, The 1800 Ma mylonite-anatectic granitoid association in Tandilia, Argentina: 7<sup>th</sup> International Conference on Basement Tectonics, Kingston, v. 7, p. 161–174.
- Dalla Salda, L. H., and Iñiguez Rodríguez, A. M., 1979, La Tinta, Precámbrico y Paleozoico de Buenos Aires: VII Congreso Geológico Argentino, Neuquén, v. 1, p. 539–550.
- De Laeter, J. R., and Kennedy, A. K., 1998, A double focusing mass spectrometer for geochronology: International Journal of Mass Spectrometry, v. 178, p. 43–50.
- De Paolo, D. J., 1988, Neodymium isotope geochemistry: An introduction. New York, NY, Springer Verlag, 187 p.
- Fernandez, R., and Echeveste, H., 1995, Caracterización geoquímica y petrológica de diques del sistema de Tandilia, Argentina: Cuartas Jornadas Geológicas y Geofísicas Bonaerenses, Junin, p. 329–337.

- Halpern, M., and Linares, E., 1970, Edad rubidio-estroncio de las rocas graníticas del basamento cristalino del área de Olavarría, provincia de Buenos Aires, República Argentina: *Revista de la Asociación Geológica Argentina*, v. 25, p. 303–306.
- Hartmann, L. A., 2002, The Mesoproterozoic Supercontinent Atlantica in the Brazilian shield—Review of geological and U-Pb zircon and Sm-Nd isotopic evidence: *Gondwana Research*, v. 5, p. 157–163.
- Hartmann, L. A., Campal, N., Santos, J. O. S., McNaughton, N. J., Bossi, J., Schipilov, A., and Lafon, J.-M., 2001, Archean crust in the Rio de la Plata Craton, Uruguay—SHRIMP U-Pb zircon reconnaissance geochronology: *Journal of South American Earth Sciences*, v. 14, p. 557–570.
- Hartmann, L. A., and Delgado, I. M., 2001, Cratons and orogenic belts of the Brazilian Shield and their contained gold deposits: *Mineralium Deposita*, v. 36, p. 207–217.
- Hartmann, L. A., Leite, J. A. D., Silva, L. C., Remus, M. V. D., McNaughton, N. J., Groves, D. I., Fletcher, I. R., Santos, J. O. S., and Vasconcellos, M. A. Z., 2000, Advances in SHRIMP geochronology and their impact on understanding the tectonic and metallogenic evolution of southern Brazil: *Australian Journal of Earth Sciences*, v. 47, p. 829–844.
- Hartmann, L. A., Piñeyro, D., Bossi, J., Leite, J., and McNaughton, N. J., 2000, Zircon U/Pb SHRIMP dating of Paleoproterozoic Isla Mala granitic magmatism in the Rio de la Plata Craton, Uruguay: *Journal of South American Earth Sciences*, v. 13, p. 105–113.
- Hartmann, L. A., Takehara, L., Leite, J. A. D., McNaughton, N. J., and Vasconcellos, M. A. Z., 1997, Fracture sealing in zircon as evaluated by electron microprobe analyses and back-scattered electron imaging: *Chemical Geology*, v. 141, p. 67–72.
- Iacumin, M., Piccirillo, E. M., Girardi, V. A. V., Teixeira, W., Bellieni, G., Echeveste, H., Fernandez, R., Pinese, J. P. P., and Ribot, A., 2001, Early Proterozoic calc-alkaline and Middle Proterozoic tholeiitic dyke swarms from Central-Eastern Argentina: Petrology, geochemistry, Sr-Nd isotopes, and tectonic implications: *Journal of Petrology*, v. 42, p. 2109–2143.
- Iñiguez, A. M., Del Valle, A., Poiré, D., Spalletti, L., and Zalba, P., 1989, Cuenca Precámbrica–Paleozoico inferior de Tandilia, Provincia de Buenos Aires, *in* Chebli, G., and Spalletti, L. A., eds., *Cuencas sedimentarias argentinas*: Instituto Superior de Correlación Geológica, Universidad Nacional de Tucumán, Serie Correlación Geológica, v. 6, p. 245–263.
- Leite, J. A. D., Hartmann, L. A., Fernandes, L. A. D., McNaughton, N. J., Soliani, Ê., Koester, E., Santos, J. O. S., and Vasconcellos, M. A. Z., 2000, Zircon U-Pb SHRIMP dating of gneissic basement of the Dom Feliciano Belt, southernmost Brazil: *Journal of South American Earth Sciences*, v. 13, p. 739–750.
- Ludwig, K. R., 1999, Using Isoplot/Ex, version 2, A geochronological toolkit for microsoft Excel: Berkeley Geochronological Center Special Publication 1a, 47 p.
- \_\_\_\_\_, 2001, Squid 1.02: A user manual: Berkeley Geochronological Center Special Publication 2, 19 p.
- Marchese, H. G., and Di Paola, E., 1975, Reinterpretación estratigráfica de la Perforación de Punta Mogotes I, Provincia de Buenos Aires: *Asociación Geológica Argentina, Reg.*, v. 1, p. 44–52.
- Pankhurst, R. J., Ramos, A., and Linares, E., 2001, Antiquity and evolution of the Rio de la Plata craton in Tandilia, southern Buenos Aires Province, Argentina: XI Congreso Latinoamericano de Geología y III Congreso Uruguayo de Geología, Montevideo, Uruguay, IGCP Symposium 436, paper 194, CD version.
- Preciozzi, F., Basei, M. A., and Masquelin, H., 1999, New geochronological data from the Piedra Alta Terrane (Rio de la Plata Craton): II South American Symposium on Isotope Geology, Carlos Paz, Argentina, p. 341–343.
- Ramos, V. A., 1988, Late Proterozoic–Early Paleozoic of South America—a collisional history: *Episodes*, v. 11, p. 168–174.
- \_\_\_\_\_, 1996, Evolución tectónica de la plataforma continental, *in* Ramos, V. A., and Turic, M. A., eds., *Geología y recursos naturales de la plataforma continental Argentina*: Buenos Aires, Argentina, Asociación Geológica Argentina and Instituto Argentino del Petróleo, p. 385–404.
- \_\_\_\_\_, 1999, Rasgos estructurales del territorio argentino. 1. Evolución tectónica de la Argentina, *in* Geología Argentina: Buenos Aires, Argentina, *Anales SEGEMAR*, v. 29, no. 24, 715–784.
- Smith, J. B., Barley, M. E., Groves, D. I., Krapez, B., McNaughton, N. J., Bickle, M. J., and Chapman, H. J., 1998, The Scholl shear zone, West Pilbara: Evidence for a terrane boundary structure from integrated tectonic analyses, SHRIMP U/Pb dating, and isotopic and geochemical data of granulitoids: *Precambrian Research*, v. 88, p. 143–171.
- Teixeira, W., Pinese, J. P. P., Iacumin, M., Girardi, V. A. V., Piccirillo, E. M., Echeveste, H., Ribot, A., Fernandez, R., Renne, P. R., and Heaman, L. M., 2001, Geochronology of calc-alkaline and tholeiitic dyke swarms of Tandilia, Rio de la Plata Craton, and their role in the Paleoproterozoic tectonics: III Symposium South American Isotope Geology, Pucón, Chile, p. 257–260.
- Teixeira, W., Renne, P. R., Bossi, J., Campal, N., and D'Agrella Filho, M. S., 1999,  $^{40}\text{Ar}/^{40}\text{Ar}$  and Rb-Sr geochronology of the Uruguayan dike swarm, Rio de la Plata Craton and implications for Proterozoic intra-plate activity in western Gondwana: *Precambrian Research*, v. 93, p. 153–180.
- Teruggi, M. E., and Kilmurray, J. O., 1980, Sierras Septentrionales de la Provincia de Buenos Aires, *in* Geología Regional Argentina: Córdoba, Argentina, Academia Nacional de Ciencias, v. II, p. 919–956.

- Teruggi, M., Kilmurray, J., and Dalla Salda, L., 1973, Los dominios tectónicos de la región de Tandil: *Anales Sociedad Científica Argentina*, v. 1-2, p. 81–94.
- \_\_\_\_\_, 1974a, Los dominios tectónicos de la región de Balcarce: *Revista de la Asociación Geológica Argentina*, v. 29, p. 265–276.
- Teruggi, M., Kilmurray, J., Rapela, C., and Dalla Salda, L., 1974b, Diques básicos en las Sierras de Tandil: *Revista de la Asociación Geológica Argentina*, v. 29, p. 41–60.
- Teruggi, M., Leguizamón, M., and Ramos, V., 1988, Metamorfitas de bajo grado con afinidades oceánicas en el basamento de Tandil: Su implicancia geotectónica, *Provincia de Buenos Aires: Revista de la Asociación Geológica Argentina*, v. 43, p. 366–374.
- Varela, R., Cingolani, C., and Dalla Salda, L., 1988, Geocronología Rb-Sr en granitoides del basamento de Tandil, Prov. De Buenos Aires, Argentina, *in* Segundas Jornadas Geológicas Bonaerenses, Bahía Blanca, Actas: Buenos Aires, Argentina, Sociedad Geológica Argentina, p. 291–305.
- Varela, R., Dalla Salda, L., and Cingolani, C., 1985, La edad Rb-Sr del Granito de Vela, Tandil, *in* Primeras Jornadas Geológicas Bonaerenses, Actas: Buenos Aires, Argentina, Sociedad Geológica Argentina, p. 123–132.

### Appendix A. Zircon Description

The 10 rock samples from the Buenos Aires Complex were selected for this SHRIMP study as representative of the Tandil, Balcarce, and Azul regions (Fig. 3; Table 1). All zircon crystals from the 10 samples are prismatic 2:1 or 3:1, which is typical of magmatic crystallizations, but nearly all have rounded terminations and complex internal structures, characteristic of solid-state recrystallization (Figs. 4 and 5). The rounding was caused by amphibolite-facies metamorphism, whereas the complex internal structures are interpreted as due to recrystallization and diffusion during the metamorphic event and during the shear zone-related metamorphism. The crystals have few fractures, which are either radial or crosscutting. Many fractures are sealed by zircon that is bright in BSE, which also occurs in patches and bands along rims or anywhere in the crystal, similar to features described by Hartmann et al. (1997) in southern Brazilian zircon crystals. Few mineral inclusions are present. Metamict portions are nearly absent, but very thin and small in the few crystals in which they occur.

Eighteen BSE images of zircon crystals from the tonalite, sample Ta1, show that most are euhedral and only a few are rounded. The internal structure of the crystals is less complex than in most other samples, because large homogeneous cores are present. Euhedral zoning is typically present along the rims. Portions that are bright in BSE occur both in the center of the crystals and along the rims.

Thirteen BSE images of zircon crystals from the Ruta 30 tonalitic gneiss, sample Ta3, show that most are prismatic, have an aspect ratio of 2:1, and show

little rounding. Radial fractures are common and thin metamict bands are present. Thirteen BSE images were made from zircon crystals from the Ruta 30 monzogranite, sample Ta4, and these show that most crystals are similar to those from sample Ta3, because they are euhedral, have an aspect ratio of 2:1, and show little rounding.

Eighteen BSE images of zircon crystals from the Chacofi quarry mafic garnet gneiss, sample Ta6, show a prismatic shape but prominent rounding of the rims. Sixteen BSE images of zircon crystals from the Chacofi quarry tonalite, sample Ta7, show a euhedral shape but considerable rounding of rims.

Eighteen BSE images of zircon crystals from the banded garnet granite, sample Ta8, are prismatic but all are rounded by metamorphism. Fractures are mostly irregular and commonly sealed by bright in BSE zircon, which extends to many portions of the crystals occupying about 10–30% of the volume of the crystals. These portions that are bright in BSE tend to be very porous, inhibiting dating by SHRIMP because of high common Pb. Only a few small metamict portions are present.

Eleven BSE images of zircon crystals from the Cerro Triunfo mafic charnockitic gneiss, sample Ta9, show an aspect ratio of 2:1, although with very prominent rounding of the crystals. Many crystals have porous rims. Seventeen BSE images of zircon crystals from the mylonitic syenogranite, sample Ta10, show a euhedral shape, but some are rounded; all have complex internal structures.

Nineteen BSE images of zircon crystals from the homogeneous charno-enderbite, sample Ta11, show a complex internal structure and prismatic shape, but exhibit well-rounded terminations because of high-grade metamorphism. A few crystals are disc-shaped or spherical. Fifteen BSE images of zircon crystals from the Villa Monica quarry grey charno-enderbite, sample Ta12, show mostly a euhedral shape, an aspect ratio of 2:1, and some rounding.